All-Fiber Chirped Microwave Pulses Generation Based on Spectral Shaping and Wavelength-to-Time Conversion

Hao Chi and Jianping Yao, *Senior Member, IEEE*

***Abstract*—An approach to generating chirped microwave pulse based on optical spectral shaping and nonlinear chromatic-dispersion-induced wavelength-to-time mapping using all-fiber components is proposed and demonstrated. In the proposed approach, the spectrum of a femtosecond pulse is shaped by a two-tap Sagnac-loop filter that has a sinusoidal spectrum response. The spectrum shaped pulse is then sent to a dispersive element that has first- and second-order chromatic dispersions. Thanks to the nonlinear wavelength-to-time mapping of the dispersive element, a temporal pulse that has a central frequency in the microwave band with a large chirp is generated, which provides the potential for applications in high-speed communications and radar systems. Numerical and proof-of-concept experimental results are presented.**

***Index Terms*—Chirped pulse, chromatic dispersion, frequency modulation, pulse shaping, radar, Sagnac-loop filter, waveform generation.**

I. Introduction

OPTICAL technology with advantageous features such as wideband width and low loss has been extensively researched for applications in high-speed communications and radars [1]. In a modern radar system, to increase the range resolution, a pulse compression technique is largely used. To achieve pulse compression, radar pulses are usually chirped or phase encoded. Chirped RF pulses can be generated in the electrical domain by using a voltage-controlled oscillator (VCO) [2], or a surface acoustic wave (SAW) dispersive delay line [3]. Chirped RF pulses can also be generated using digital electronic circuits [4]. The major difficulty associated with the above techniques for chirped RF pulse generation is that the central frequency of the generated chirped pulse is limited to a few gigahertz. For many applications, the central frequency should be in the tens or hundreds of gigahertz bands [5].

To generate electrical pulses with a high central frequency, optical techniques are usually used. Among the numerous approaches, spatial light modulator (SLM)-based pulse shaping has been widely adopted [6], [7], in which arbitrary RF pulses are generated by modulating the spatially dispersed spectrum of an input ultrashort optical pulse at the SLM. The key advantage of the SLM-based approaches is that the SLM can be updated in real time, which makes the generation of arbitrary electrical pulses possible. The major difficulty associated with an SLM-based pulse-shaping system is that the system requires fiber-to-space and space-to-fiber coupling, which makes the system bulky and complicated. To generate high-frequency chirped pulses without using free space optics, Zeitouny *et al.* [8] proposed a method using pure fiber-optic components. This approach is based on the interference of two optical pulses that are reflected from two chirped fiber Bragg gratings (CFBGs) with different chirp rates. Depending on the chirp rate difference between the two CFBGs, a chirped RF pulse with a different chirp rate was generated. The central frequency of the chirped pulse can also be adjusted by tuning the time delay between the two reflected chirped optical pulses. The major advantage of this approach is that the system is implemented using pure fiber-optic devices, which has the potential for integration using photonic integrate circuit technology. High-frequency phase-coded pulses can also be generated using pure fiber-optic components. We recently proposed an approach to generating phase-coded microwave pulses using a mode-locked fiber laser and a fiber-based unbalanced Mach–Zehnder interferometer (MZI) [9], in which the phase coding was realized using an optical phase modulator that was incorporated in one arm of the MZI.

It is known that a temporal pulse can be generated based on wavelength-to-time mapping in a dispersive element. If the dispersive element has only the first-order dispersion, the temporal pulse would have an envelope that is a scaled version of the spectrum profile of the spectrum-shaped pulse [10]. Based on this concept, we have recently demonstrated a system to generate microwave and millimeter-wave signals for radio-over-fiber (RoF) applications [11]. In the approach, a femtosecond pulse is spectrum shaped by a two-tap Sagnac-loop filter that has a sinusoidal spectral response. A temporal pulse is generated through wavelength-to-time mapping in a first-order-only dispersive element. A temporal pulse signal with a sinusoidal carrier that has a frequency in the millimeter-wave frequency

Manuscript received November 26, 2006; revised June 25, 2007. This work was supported by The Natural Sciences and Engineering Research Council of Canada. The work of H. Chi was supported in part by the National Natural Science Foundation of China under Grant 60407011 and by the Zhejiang Provincial Natural Science Foundation of China under Grant Y104073.

H. Chi is with the Department of Information and Electronic Engineering, Zhejiang University, Hangzhou 310027, China, and also with the Microwave Photonics Research Laboratory, School of Information Technology and Engineering, University of Ottawa, Ottawa, ON, Canada K1N 6N5.

J. Yao is with the Microwave Photonics Research Laboratory, School of Information Technology and Engineering, University of Ottawa, Ottawa, ON, Canada K1N 6N5 (e-mail: jpyao@site.uOttawa.ca).

Color versions of one or more of the figures in this paper are available online at http://ieeexplore.ieee.org.

Digital Object Identifier 10.1109/TMTT.2007.904084

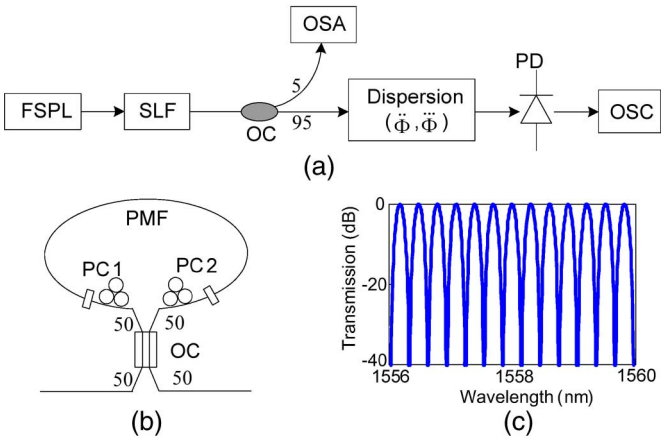

Fig. 1. Chirped microwave pulse generation based on nonlinear wavelength-to-time mapping. (a) System configuration. (b) Two-tap Sagnac-loop filter. (c) Intensity transmission of the Sagnac-loop filter. $\dot{\Phi}$ and $\ddot{\Phi}$ are, respectively, the first- and second-order dispersions in the dispersive element. (femtosecond pulse laser: FSPL; Sagnac-loop filter: SLF; optical coupler: OC; photodetector: PD; oscilloscope: OSC; polarization maintaining fiber: PMF; polarization controller: PC.

band is generated. Since the RF carrier of the pulse is pure sinusoidal, it is suitable for RoF communications applications. However, for the same system in [11], if the dispersive element also has a second-order dispersion, the carrier of the temporal pulse would be chirped. In this paper, we propose to generate chirped microwave pulses based on spectral shaping and wavelength-to-time conversion using a dispersive element with both first- and second-order dispersions for potential applications in high-speed communications and radar systems. The remainder of this paper is organized as follows. In Section II, an all-fiber pulse-shaping system to generate chirped microwave pulses is provided. In Section III, an approximate model to characterize the instantaneous frequency of the generated pulse is then presented. Numerical and experiment results are provided in Section IV. A conclusion is drawn in Section V.

II. System Configuration

The proposed chirped microwave pulse generation system is shown in Fig. 1. It consists of a femtosecond pulsed laser (FSPL), a two-tap Sagnac-loop filter, a dispersive element that has both first- and second-order dispersions, and a high-speed photodetector (PD). A femtosecond pulse generated from the FSPL is first spectrum shaped by the two-tap Sagnac-loop filter. It is known that a two-tap Sagnac-loop filter has a frequency response that is sinusoidal. The spectrum shaped pulse is then sent to the dispersive element to perform wavelength-to-time mapping. Thanks to the second-order dispersion of the dispersive element, a chirped microwave pulse with a chirp rate dependent on the value of the second-order dispersion is generated. In the proposed approach, the central frequency of the chirped pulse is determined by the value of the first-order dispersion. Therefore, by designing a dispersive element with the desired values of first- and second-order dispersions, a chirped microwave pulse with the required central frequency and the chirp rate can be generated.

III. Approximate Model

Wavelength-to-time mapping using a dispersive element has been used to generate optical pulses with arbitrary waveforms [6], [9]. In an arbitrary waveform generation system based on wavelength-to-time mapping, spectrum shaping should be implemented first. The spectrum shaping can be implemented in free space using an SLM-based configuration [6], [7]; it can also be realized using a fiber-based optical filter [9]. The linear wavelength-to-time mapping is realized by using a linear dispersion device. Assume that the intensity spectrum profile of a spectrum-shaped pulse is $S(\omega)$, after wavelength-to-time mapping in a linearly dispersive element, an electrical current $i(t)$ is generated at the output of a PD, which has a shape that is a scaled version of $S(\omega)$. The linear wavelength-to-mapping can also be explained by the so-called time-domain Fraunhofer diffraction [12].

The linear mapping relation comes from the linear group-delay expression of a linear dispersion medium $t = d\Phi(\omega)/d\omega = \dot{\Phi} + \ddot{\Phi}(\omega - \omega_0)$, where $\Phi(\omega)$ is the spectral phase of the transfer function of the linear dispersion element, $\dot{\Phi} = d\Phi(\omega)/d\omega|_{\omega=\omega_0}$ is the mean group delay, and $\ddot{\Phi} = d^2\Phi(\omega)/d\omega^2|_{\omega=\omega_0}$ is the first-order dispersion.

In our system, however, a dispersive element having second-order dispersion is employed to achieve nonlinear wavelength-to-time mapping for the generation of chirped microwave pulses. A strict analysis on the propagation of a spectrum-shaped femtosecond pulse in a dispersive element with higher order dispersions is extremely complicated [13]. Therefore, in this paper, a simplified treatment based on nonlinear wavelength-to-time mapping is employed in which the dispersive element having both first- and second-order dispersions is considered.

In the configuration shown in Fig. 1(a), the optical spectrum shaping is realized using a Sagnac-loop filter. Since a single section of polarization maintaining fiber (PMF) is used, the Sagnac-loop filter is a two-tap filter with an intensity transfer function given by $1 + \cos(\omega t_0)$, where t_0 is the time-delay difference between the two optical paths along the fast and slow axes determined by the birefringence and the length of the PMF [14].

For simplicity, we assume that the input ultrafast pulse is a Dirac delta function $\delta(t)$. Therefore, the intensity spectrum of the shaped pulse at the output of the Sagnac-loop filter is given by

$$S(\omega) = 1 + \cos(\omega t_0). \tag{1}$$

On the other hand, the group delay of the pulse passing through the dispersive element $t(\omega)$, if only the first- and second-order dispersions are considered, can be expressed as

$$t(\omega) = \frac{d\Phi(\omega)}{d\omega} = \dot{\Phi} + \ddot{\Phi}\omega + \frac{1}{2}\dddot{\Phi}\omega^2 \tag{2}$$

where $\Phi(\omega)$ is the spectral phase of the transfer function of the dispersive element $H(\omega) = |H(\omega)|\exp\{-j\Phi(\omega)\}$, $\dot{\Phi}$, $\ddot{\Phi}$, and $\dddot{\Phi}$ denote the mean group delay, first-order dispersion, and second-order dispersion, respectively. Note that ω is the relative angular frequency with respect to the central frequency of the

pulse. According to (2), the nonlinear time-to-frequency mapping relation can be expressed as

$$\omega(t) = \frac{-\ddot{\Phi} \pm \sqrt{\ddot{\Phi}^2 + 2\dddot{\Phi}(t - \dot{\Phi})}}{\dddot{\Phi}} \tag{3}$$

where the sign $\pm$ corresponds to the cases of positive and negative $\ddot{\Phi}$, respectively. For simplicity, we use t to replace the term of relative time delay $t - \dot{\Phi}$ in the following expressions. After the signal propagates through the dispersion medium and is detected by the PD, the spectral waveform is mapped into a time-domain waveform as $S(\omega) \rightarrow i(t)$, and $i(t)$ is given by

$$\begin{aligned} i(t) &\propto 1 + \cos[\omega(t)t_0] \\ &= 1 + \cos[\Psi(t)] \\ &= 1 + \cos\left(\frac{\sqrt{\ddot{\Phi}^2 + 2\dddot{\Phi}t}}{\dddot{\Phi}}t_0 + \phi\right) \end{aligned} \tag{4}$$

where $\phi = \pm\ddot{\Phi}t_0/\dddot{\Phi}$ is a constant phase.

The obtained signal current $i(t)$ is a continuous wave since the input ultrafast pulse is assumed to be a Dirac delta function. In fact, if the input pulse has a nonzero width, the width of the output waveform is time limited. Taking into account the nonzero width of the input pulse, the detected temporal waveform should be confined in an envelope, which can be written as

$$i(t) \propto r(t) \cdot \left[1 + \cos\left(\frac{\sqrt{\ddot{\Phi}^2 + 2\dddot{\Phi}t}}{\dddot{\Phi}}t_0 + \phi\right)\right] \tag{5}$$

where $r(t)$ is the pulse envelope. Assuming that the input short pulse is Gaussian shaped as $g(t) = \exp(-t^2/\tau_0^2)$, where τ_0 is the half-width at $1/e$ maximum, the output pulse envelope $r(t)$ can be analytically expressed using the Airy function. Regarding the detailed analysis of the property of $r(t)$, readers may refer to [15] and [16]. It is known that for a small $\dddot{\Phi}$, the output pulse envelope $r(t)$ is approximately Gaussian with only a slight shift of the pulse peak, with a pulsewidth of $|\ddot{\Phi}|/\tau_0$ [17].

The instantaneous RF carrier frequency of the waveform can be written as

$$\omega_{rf}(t) = \frac{d\Psi(t)}{dt} = (\ddot{\Phi}^2 + 2\dddot{\Phi}t)^{-1/2} \cdot t_0. \tag{6}$$

It is shown that the waveform is nonlinearly chirped. The central frequency at $t = 0$ can be calculated to be $\omega_0 = t_0/|\ddot{\Phi}|$, which means that the central frequency of the generated chirped pulse is only dependent upon the first-order dispersion for a two-tap Sagnac-loop filter with a given time delay different t_0. The ratio $\ddot{\Phi}t_0/|\ddot{\Phi}|^3$ determines the chirp rate of the generated pulse, which can be seen more directly from the first-order approximation of (6) as follows:

$$\omega_{rf} \cong \frac{t_0}{\ddot{\Phi}} - \frac{\dddot{\Phi}t_0}{|\ddot{\Phi}|^3}t. \tag{7}$$

Therefore, a microwave pulse with the required central frequency and the chirp rate can be generated using the proposed system by selecting a dispersive element with suitable first- and second-order dispersions. It should be noted that a linear frequency modulation is not always necessary in a pulse-compression radar. The frequency modulation can be of almost any form, provided that the pulse compression filter is designed to match the transmitted waveform.

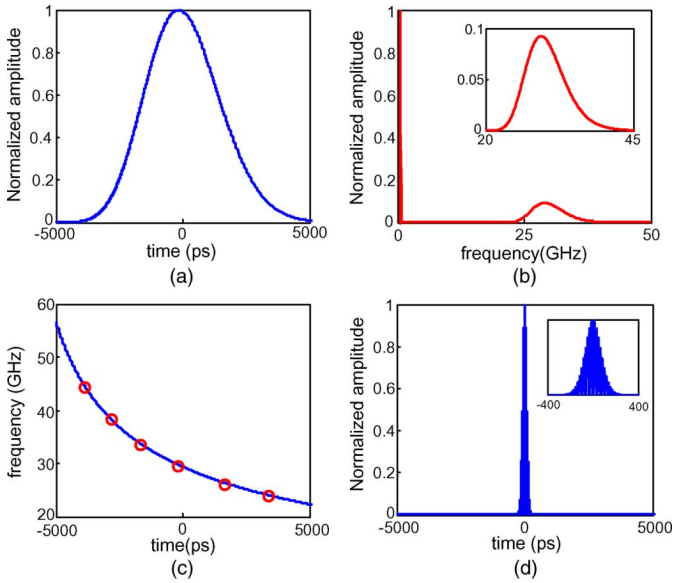

Fig. 2. Numerical results, $\ddot{\Phi} = 440$ ps^2, $\dddot{\Phi} = 14$ ps^3, $\omega_0/2\pi = 29$ GHz. (a) Envelope of the generated pulse. (b) Spectrum (inset: zoom-in display). (c) Instantaneous frequency versus time (solid line: predicted by (6), circle: obtained from numerical result). (d) Compressed pulse obtained by autocorrelation (inset: zoom-in display).

IV. Results and Discussions

Numerical simulations and a proof-of-concept experiment are implemented to verify the proposed approach. In the numerical simulations, we use a transform-limited Gaussian pulse with a full width at half maximum (FWHM) of 350 fs. The central wavelength of the optical pulse is 1558 nm. The free spectral range (FSR) of the Sagnac-loop filter is 0.1 nm, which corresponds to a time-delay difference t_0 of 80.9 ps. The first-order dispersion $\ddot{\Phi}$ is chosen to be 440 ps^2. Therefore, the central frequency of the generated waveform is calculated to be approximately 29 GHz.

In the first numerical simulation, the second-order dispersion $\dddot{\Phi}$ is set to be 14 ps^3. The simulation results are shown in Fig. 2. The envelope of the generated chirped pulse is shown in Fig. 2(a), which is close to a Gaussian pulse with a slight asymmetry. The electrical spectrum of the pulse is shown in Fig. 2(b), in which the sideband is broadened thanks to the frequency chirping induced by the second-order dispersion. The instantaneous frequency versus time of the chirped pulse obtained from the numerical result by a Hilbert transform [18] is shown in Fig. 2(c), which matches well with the prediction given by (6). According to the temporal waveform and its spectrum, the time-bandwidth product of the generated chirped pulse is estimated to be around 26.0. Fig. 2(d) shows the compressed pulse,

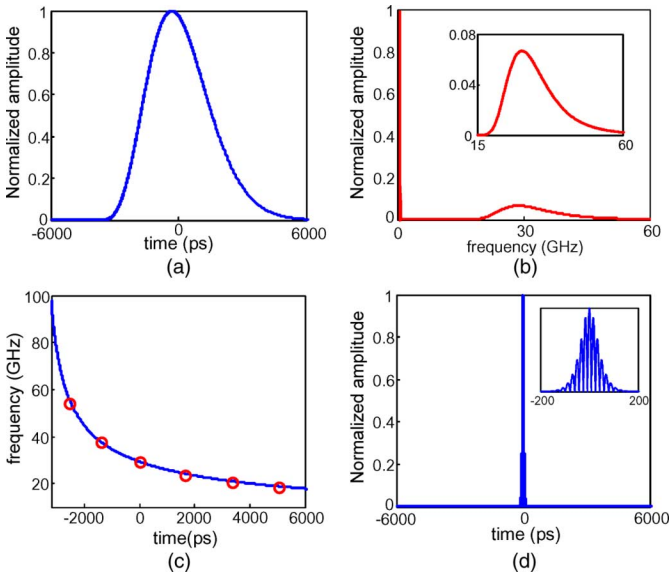

Fig. 3. Numerical results, $\ddot{\Phi} = 440$ ps^2, $\dddot{\Phi} = 28$ ps^3, $\omega_0/2\pi = 29$ GHz. (a) Envelope of the generated pulse. (b) Spectrum (inset: zoom-in display). (c) Instantaneous frequency versus time (solid line: prediction by (6), circle: obtained from numerical result). (d) Compressed pulse obtained by autocorrelation (inset: zoom-in display).

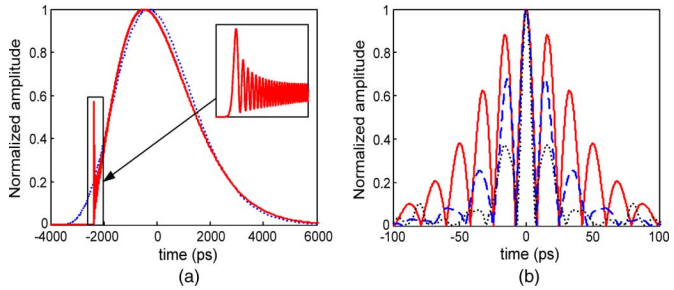

Fig. 4. Numerical results, $\ddot{\Phi} = 440$ ps^2, $\omega_0/2\pi = 29$ GHz. (a) Solid: waveform envelope for $\dddot{\Phi} = 42$ ps^3, dotted: waveform envelope for $\dddot{\Phi} = 28$ ps^3. (b) Autocorrelation waveforms, solid: $\dddot{\Phi} = 28$ ps^3, dashed: $\dddot{\Phi} = 42$ ps^3, dotted: $\dddot{\Phi} = 56$ ps^3.

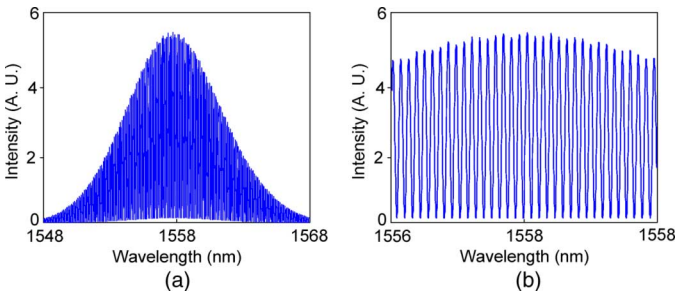

Fig. 5. (a) Filtered optical spectrum of the femtosecond laser pulse by the Sagnac-loop filter. (b) Zoom-in display of (a).

which is obtained by calculating the autocorrelation of the generated chirped pulse (equivalent to matched filtering). By comparing the FWHM widths of the waveforms in Fig. 2(a) and (d), the compression ratio is estimated to be around 23.9.

In the second numerical simulation, we change $\dddot{\Phi}$ to be 28 ps^3. Simulation results are shown in Fig. 3. The envelope of the generated chirped pulse is shown in Fig. 3(a). It is seen that the pulse envelope is more asymmetrical compared to that shown in Fig. 2(a) due to a larger second-order dispersion in this case. The larger $\dddot{\Phi}$ also leads to a greater spectrum broadening, as shown in Fig. 3(b). The time-bandwidth product and the compression ratio in this case are estimated to be around 43.3 and 47.0, respectively. Again, the instantaneous frequency versus time, as shown in Fig. 3(c), is identical to the prediction given by (6). Therefore, the effectiveness of the given theoretical model for characterizing the generated chirped microwave pulses is verified.

To generate pulses with a larger time-bandwidth product (i.e., larger chirping rate), a large second-order dispersion $\ddot{\Phi}$ is required. However, a higher $\ddot{\Phi}$ would lead to unexpected ripples in the generated waveforms. As shown in Fig. 4(a), strong ripples are observed at the left side of the generated waveform when a larger $\ddot{\Phi}$ is used, where $\dddot{\Phi}$ is set to be 42 ps^3 while keeping $\ddot{\Phi}$ as 440 ps^2. The zoom-in display of the oscillating part is shown in the inset of Fig. 4(a). For comparison, the pulse envelope for $\dddot{\Phi} = 14$ ps^3 is also shown in Fig. 4(a) (the dotted curve). These unwanted ripples would degrade the pulse compression performance. We find, however, that the major spectral components of these ripples are higher than 100 GHz, which can be removed by using a low-pass filter. Fig. 4(b) shows the autocorrelation results, where $\dddot{\Phi}$ are 28, 42, and 56 ps^3, respectively. Note that we have filtered out the oscillating part in the generated waveforms before performing the autocorrelation. It is shown that a higher $\dddot{\Phi}$ leads to better suppression of the autocorrelation sidelobes, which is important to improve the range resolution of a radar system. In the case of $\dddot{\Phi} = 56$ ps^3, the first sidelobe of the autocorrelation waveform is suppressed to below the half maximum of the main peak, shown as the dotted curve in Fig. 4(b). In this case, the pulse compression ratio is as high as 410, obtained by comparing the FWHM of the generated chirped pulse and the FWHM of the autocorrelation waveform.

An experiment based on the setup shown in Fig. 1 is then performed to verify the proposed chirped pulse generation method. Due to the lack of a dispersive element with a high second-order dispersion, in the experiment we use a length of 20-km standard single-mode fiber (SSMF) as a dispersion element. The first- and second-order dispersions $\ddot{\Phi}$ and $\dddot{\Phi}$ of the SSMF are approximately 446 ps^2 and 0.8 ps^3, respectively. A femtosecond pulse laser with an FWHM of 350 fs and a central wavelength of 1558 nm is used as the ultrashort pulse source. The time-delay difference t_0 of the Sagnac-loop filter is set to be around 67.5 ps (which is equivalent to an FSR of 0.12 nm in the 1558-nm band). The filtered optical spectrum of the femtosecond laser pulse by the Sagnac-loop filter is shown in Fig. 5(a) with a zoom-in display shown in Fig. 5(b). The central frequency of the generated microwave pulse is estimated to be around 24 GHz based on (6). The experimental results are shown in Fig. 6. As can be seen from Fig. 6(a), the FWHM of the generated pulse is around 4.4 ns, which is measured by using a sampling oscilloscope. The spectrum of the pulse is given in Fig. 6(b). The FWHM of the spectrum is around 0.7 GHz. Therefore, the time-bandwidth product is estimated to be around 3.1. Fig. 6(c) shows the instantaneous frequency versus time, where the circles are the experimental results and the solid curve is the theoretical prediction according to (6). A good agreement between

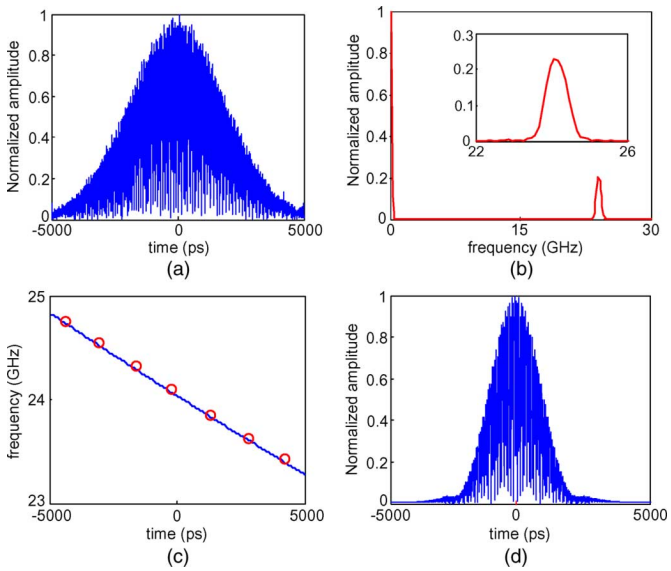

Fig. 6. Experimental results. (a) Generated pulse. (b) Spectrum (inset: zoom-in display). (c) Instantaneous frequency versus time (solid line: prediction by (6), circle: obtained from experimental result. (d) Compressed pulse obtained by autocorrelation.

the experimental results and the theoretical prediction is observed. Fig. 6(d) shows the autocorrelation result of the generated chirped pulse, the FWHM of which is around 1.7 ns. Therefore, a pulse compression ratio of 2.6 is achieved.

Despite that the time-bandwidth product of the generated pulse and the achieved compression ratio are low due to the limited second-order dispersion in the SSMF, the second-order dispersion-induced pulse chirping is observed and verified by the experimental results, which also agree well with the theoretical predictions.

For practical applications where a high pulse compression ratio is required, a dispersive element with a high second-order dispersion is necessary. A possible solution is to use a fiber Bragg grating (FBG) with both first- and second-order dispersions (nonlinearly CFBG) [19]. The central frequency and chirp rate of the generated chirped pulse are determined, respectively, by the first- and second-order dispersions. Another solution is to use a specially designed photonic crystal fiber (PCF) that has a larger second-order dispersion. Up to now, several types of PCFs with different dispersion properties have been successfully designed for different applications [20], [21]. It is known that the large tailorability in the design of the PCFs, by controlling the air-hole sizes, shapes, and arrangements, provides a fruitful means to tune the dispersion curve to obtain the expected dispersion properties.

We have recently demonstrated the generation of 18- and 36-GHz pulses using a similar setup in Fig. 1 [11]. The key difference between this approach and the approach in [11] is that the approach here can generate a chirped microwave pulse based on nonlinear wavelength-to-time mapping, while the approach in [11] can only generate a pure sinusoidal microwave pulse (without chirping), which was based on linear wavelength-to-time mapping. From the results given here, it is clear that to generate nonchirped microwave pulses based on the wavelength-to-time mapping technique, the higher order dispersions in the dispersive element should be eliminated or kept as small as possible.

V. Conclusion

We have proposed a method for the generation of chirped microwave pulses based on optical spectral shaping and nonlinear wavelength-to-time mapping. In the proposed system, the spectrum shaping was implemented using a two-tap Sagnac-loop filter with a sinusoidal spectrum profile. The chirped microwave pulse was then generated using a dispersive element with both first- and second-order dispersions. The first-order dispersion determines the central frequency and the second-order dispersion determines the chirp rate. The key advantage of this approach is that the system can be implemented using all-fiber components, which has the potential for integration. The effectiveness of the approach was verified via numerical simulations and a proof-of-concept experiment. Chirped pulses with a central frequency of 24 GHz were experimentally generated and a pulse compression of approximately 2.6 was demonstrated. To achieve a high compression ratio for practical applications, a dispersive element with a much higher second-order dispersion is required, which could be realized by using a nonlinearly CFBG or a specially designed PCF with a high second-order dispersion. The numerical results showed that a compression ratio as high as 410 could be achieved if a dispersive element with a first-order dispersion of 440 ps^2 and a second-order dispersion of 56 ps^3 is available. The approach offers a potential solution for chirped pulse generation with high central frequency and large time-bandwidth product for applications in pulse-compression radar systems.

References

[1] H. Zmuda and E. N. Toughlian, *Photonic Aspects of Modern Radar*. Boston, MA: Artech House, 1994.
[2] H. Kwon and B. Kang, "Linear frequency modulation of voltage-controlled oscillator using delay-line feedback," *IEEE Microw. Wireless Compon. Lett.*, vol. 15, no. 6, pp. 431–433, Jun. 2005.
[3] A. M. Kawalec, "SAW dispersive delay lines in radar signal processing," in *IEEE Int. Radar Conf.*, May 1995, pp. 732–736.
[4] H. D. Griffiths and W. J. Bradford, "Digital generation of high time-bandwidth product linear FM waveforms for radar altimeters," *Proc. Inst. Elect. Eng.—Radar and Signal Processing*, vol. 139, no. 2, pt. F, pp. 160–169, Apr. 1992.
[5] M. I. Skolnik, *Introduction to Radar*. New York: McGraw-Hill, 1962.
[6] J. Chou, Y. Han, and B. Jalali, "Adaptive RF-photonic arbitrary waveform generator," *IEEE Photon. Technol. Lett.*, vol. 15, no. 4, pp. 581–583, Apr. 2003.
[7] J. D. McKinney, D. E. Leaird, and A. M. Weiner, "Millimeter-wave arbitrary waveform generation with a direct space-to-time pulse shaper," *Opt. Lett.*, vol. 27, no. 15, pp. 1345–1347, Aug. 2002.
[8] A. Zeitouny, S. Stepanov, O. Levinson, and M. Horowitz, "Optical generation of linearly chirped microwave pulses using fiber Bragg gratings," *IEEE Photon. Technol. Lett.*, vol. 17, no. 3, pp. 660–662, Mar. 2005.
[9] H. Chi and J. P. Yao, "An approach to photonic generation of high-frequency phase-coded RF pulses," *IEEE Photon. Technol. Lett.*, vol. 19, no. 5, pp. 768–770, May 2007.
[10] B. Jalali, J. Chou, and Y. Han, "Optically sculpt UWB waveforms," *Microw. RF Mag.*, vol. 43, no. 8, pp. 54–62, Aug. 2004.
[11] H. Chi, F. Zeng, and J. P. Yao, "Photonic generation of microwave signals based on pulse shaping," *IEEE Photon. Technol. Lett.*, vol. 19, no. 5, pp. 668–670, May 2007.
[12] M. A. Muriel, J. Azana, and A. Carballar, "Real-time Fourier transformer based fiber grating," *Opt. Lett.*, vol. 24, no. 1, pp. 1–3, Jan. 1999.

[13] W. Zhao and E. Bourkoff, "Femtosecond pulse propagation in optical fibers: Higher order effects," *IEEE J. Quantum Electron.*, vol. 24, no. 2, pp. 365–372, Feb. 1988.
[14] X. Fang and R. O. Claus, "Polarization-independent all-fiber wavelength-division multiplexer based on a Sagnac interferometer," *Opt. Lett.*, vol. 20, no. 20, pp. 2146–2148, Oct. 1995.
[15] M. Miyagi and S. Nishida, "Pulse spreading in a single-mode fiber due to third-order dispersion," *Appl. Opt.*, vol. 18, no. 5, pp. 678–682, Mar. 1979.
[16] M. Amemiya, "Pulse broadening due to higher order dispersion and its transmission limit," *J. Lightw. Technol.*, vol. 20, no. 4, pp. 591–597, Apr. 2002.
[17] G. P. Agrawal, *Nonlinear Fiber Optic*. San Diego, CA: Academic, 1989.
[18] B. Boashash, "Estimating and interpreting the instantaneous frequency of a signal—Part 1: Fundamentals," *Proc. IEEE*, vol. 80, no. 4, pp. 520–538, Apr. 1992.
[19] T. Komukai and M. Nakazawa, "Fabrication of non-linearly chirped fiber Bragg gratings for higher-order dispersion compensation," *Opt. Commun.*, vol. 154, no. 1, pp. 5–8, Aug. 1998.
[20] D. Mogilevtsev, T. A. Birks, and P. S. J. Russell, "Group-velocity dispersion in photonic crystal fibers," *Opt. Lett.*, vol. 23, no. 21, pp. 1662–1664, Nov. 1998.
[21] J. C. Knight, J. Arriaga, T. A. Birks, A. Ortigosa-Blanch, W. J. Wadsworth, and P. S. J. Russell, "Anomalous dispersion in photonic crystal fiber," *IEEE Photon. Technol. Lett.*, vol. 12, no. 7, pp. 807–809, Jul. 2000.

Hao Chi received the Ph.D. degree in electronic engineering from Zhejiang University, Hangzhou, China, in 2001.

In 2003, he joined the Department of Information and Electronic Engineering, Zhejiang University. Prior to that, he spent a half year with the Hong Kong Polytechnic University, as a Research Assistant, and two years with Shanghai Jiaotong University, as a Post-Doctoral Fellow. Since July 2006, he has also been with the Microwave Photonics Research Laboratory, University of Ottawa, Ottawa, Ontario, Canada. His research interests include optical communications and networking, microwave photonics, fiber-optic sensors, and optical signal processing.

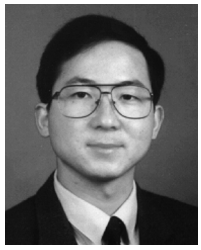

Jianping Yao (M'99–SM'01) received the Ph.D. degree in electrical engineering from the Université de Toulon, Toulon, France, in 1997.

From 1999 to 2001, he held a faculty position with the School of Electrical and Electronic Engineering, Nanyang Technological University, Singapore. In 2001, he joined the School of Information Technology and Engineering, University of Ottawa, Ottawa, Ontario, Canada, where he is currently a Professor and Director of the Microwave Photonics Research Laboratory. He is a Guest Professor with Shantou University, Shantou, China, and Sichuan University, Sichuan, China. In 2005, he was an Invited Professor with the Institut National Polytechnique de Grenoble, Grenoble, France. He has authored or coauthored over 160 papers in refereed journal and conference proceedings. His research has focused on microwave photonics, which includes all-optical microwave signal processing, photonic generation of microwave, millimeter-wave, and terahertz, RoF, UWB-over-fiber, FBGs for microwave photonics applications, and optically controlled phased-array antennas. His research interests also include fiber lasers, fiber-optic sensors, and bio-photonics.

Dr. Yao is a member of The International Society for Optical Engineers (SPIE) and the Optical Society of America (OSA). He is a Senior Member of the IEEE Lasers and Electro-Optics Society (IEEE LEOS) and the IEEE Microwave Theory and Techniques Society (IEEE MTT-S).